Agricultural Journal 5 (6): 322-328, 2010
ISSN: 1816-9155

Energy Transmission via an Inductive Link in an Implantable System Through Macromodel

[1]M. Chaoui, [1]H. Ghariani, [1]M. Lahiani and [2]R. Perdriau
[1]Laboratory of Electronics and Information Technologies (LEIT),
Sfax National School of Engineering, BPW 3038, Tunisia
[2]ESEO-4, Rue Merlet-de-la-Boulaye, BP 30926-49009 Angers Cedex 01, France

Abstract: This study presents a macromodel-based electrical simulation model of a skin-implantable system, capable of transmitting RF power and data through an inductive link. This model makes it possible to assess the efficiency of energy transmission as a function of lateral and longitudinal displacements between the external coil (transmitter) and the implanted coil (receiver). This model must describe the behaviour of the mutual inductance in relation to lateral and longitudinal displacements. For that, a behavioural modelling was made on the basis of the mathematical equation of the mutual inductance. A polynomial interpolation of order four of this equation was established to lead to the electric model in the form of a sub circuit. This modelling made it possible to study and to simulate the efficiency and the impedance brought back to the entry of the inductive link in relation to lateral and longitudinal displacements. The power amplifier itself is a class E amplifier optimized in both output voltage and efficiency and bears an excellent tolerance to displacements.

Key words: Inductive link, RF, class E amplifier, modeling, rectifier, France

INTRODUCTION

Body-implantable electronic systems often use an inductive link for power supply and data transmission (Vandevoorde and Puers, 2001; Catrysse *et al*., 2004; Zierhofer and Hochmair, 1990). The communication between the internal and the external part of these systems has thus to be as efficient as possible as far as energy and transmission rate are concerned. Furthermore for most of these long-duty implantable devices, an inductive powering system is preferable instead of batteries for surgical and reliability issues. It has been demonstrated that two kinds of geometries can enhance the overall power efficiency of such a RF link (Zierhofer and Hochmair, 1990), especially in the case of high frequencies and external transmitter losses (Sokal and Sokal, 1975).

In this study, a novel mathematical analysis of a RF inductive link extends existing studies to the case of very low coupling factors. It takes into account the parasitic resistance of the coils which proves to be critical, especially in the case of micro-coils (Chaoui *et al*., 2002).

In any case, the amount of energy transferred to the secondary winding greatly depends on the coupling factor which ultimately defines the voltage gain, the power yield of the link and the tolerance of the system to lateral and longitudinal misalignments. An electrical model of the inductive link, taking into account lateral and longitudinal displacements through an approximated computation of this coupling factor is thus proposed. A comparison of theoretical results and electrical simulation results given by OrCAD® will then be performed.

DESIGN OF AN INDUCTIVE LINK FOR TRANSCUTANEOUS TRANSMISSION

Many different combinations of two given coil geometries have been studied in terms of stability and mutual inductance, including simple geometries such as two circular coils and more complex ones such as two solenoids, a circular coil and an Archimedes coil and a solenoid and an Archimedes coil. Indeed within the literature (Chaoui *et al*., 2003, 2005; Galbraith *et al*., 1987), the case of two Archimedes coils is adopted as an optimal case since it presents a remarkable mutual inductance. However, through rigorous calculations, better stability can be obtained with two solenoids than with two Archimedes coils only with a slight drop-off of the mutual inductance. To sum up, it has been shown that a good trade-off between stability and mutual inductance is achieved through the use of an Archimedes coil and a solenoid.

Corresponding Author: M. Chaoui, Laboratory of Electronics and Information Technologies (LEIT),
Sfax National School of Engineering, BPW 3038, Tunisia

For stability reasons, it has been demonstrated that the receiver radius b must be lower than the transmitter radius a. Figure 1 shows the representation of the association between a solenoid and an Archimedes coil. The case of a solenoid as an emitter and an Archimedes coil as a receiver presents a remarkable stability and a slightly less pronounced mutual inductance than that of the opposite case (Chaoui *et al*., 2005).

This link consists of a serial tuned transmitter and parallel tuned receiver circuits which are magnetically coupled is shown by Fig. 2 where L-R circuit with values as shown in Table 1. Figure 2 shows an equivalent circuit of an inductive link for transcutaneous power and data transfer, showing a typical voltage-in voltage-out link configuration (Chaoui *et al*., 2003, 2005; Galbraith *et al*., 1987). This link consists of a serial tuned transmitter and a parallel tuned receiver circuit which are magnetically coupled.

L_1 is the external (emitter) coil inductance and L_2 is the internal (receiver) coil inductance. Resistor R_1 is the output resistance of the RF-amplifier driving the link, including the resistance which determines the resonant circuit quality factor Q_1. The R_p resistor includes the load and the resistance of the resonant circuit quality factor Q_2.

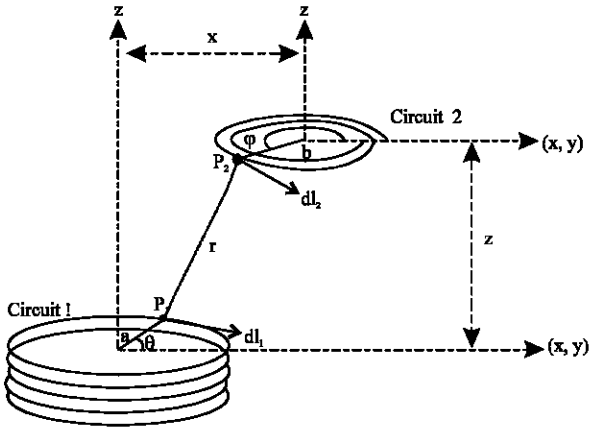

Fig. 1: Layout of a solenoid (radius a) and an archimedes coil (radius b) distant of z (longitudinally) and x (laterally)

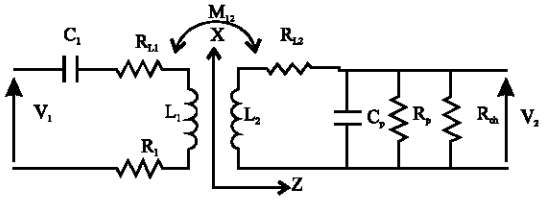

Fig. 2: Schematic of a transponder system for RF power and data transmission

R_{L1}, R_{L2}, Q_1 and Q_2, respectively represent the series resistances of the coils and the quality factors of the transmitter and the receiver. z and x are the corresponding longitudinal and lateral displacements, respectively.The models of the transmitter and receiver coils are respectively a series and a parallel L-R circuit whose values are shown in Table 1. Coil losses are represented by the parallel resistor R_{p2}. Series and parallel coil inductance and resistance are linked together by Eq. 1 and 2:

$$L_{p2} = L_2 + \frac{R_{L_2}^{\ 2}}{L_2\omega^2} \tag{1}$$

and

$$R_{p2} = R_{L_2} + \frac{(L_2\omega)^2}{R_{L_2}} \tag{2}$$

A new theoretical analysis of this particular case was performed extending the current theoretical studies, adding the impact of the parasitic coil resistances to the equations. This was achieved through a MathCAD® program that helps significantly the RF-link designer.

In order to determine the overall two-port matrix describing the inductive link, the emitter-receiver circuit containing all coupled coils is evaluated (Zierhofer and Hochmair, 1990). Coil L_1 is coupled to coil L_{p2} with the mutual inductance M(z, x). Then, the impedance matrix Z of the inductive link is calculated:

$$Z(f,z,x) = j.\omega\begin{pmatrix} L_1 & M_{12}(z,x) \\ M_{12}(z,x) & L_{p2} \end{pmatrix} \tag{3}$$

This matrix is transformed into the hybrid matrix H(f, z, x) with Eq. 4:

$$H(f,z,x) = \begin{pmatrix} H_{11} & H_{12} \\ H_{21} & H_{22} \end{pmatrix} = \frac{1}{Z_{22}(f)} \cdot \begin{pmatrix} \det Z(f,z,x) & Z_{12}(f,z,x) \\ -Z_{12}(f,z,x) & 1 \end{pmatrix} \tag{4}$$

Table 1: Coil parameters

Factors	Emitter coil	Receiver coil
Coil shape	Solenoid	Archimedes turn
Number of turns N_i	5	2
Diameter (mm)	30	20
Inductance at 10 MHz	1.54 μH	198.45 nH
Series resistance at 10 MHz	0.527 Ω	0.361 Ω
Operating frequency	10 MHz	10 MHz
Nominal displacement	x = 2-8 mm z = 4-16 mm	-

The final result is given by Eq. 5 where R_2 represents the equivalent parallel resistance of R_{p2}, R_p and R_{Load} and R_{sL1} is R_{L1} and R_1 in series:

$$H(f,z,x)=\begin{pmatrix} j\cdot\omega\cdot\dfrac{L_1L_{p2}-M_{12}(z,x)^2}{L_{p2}}+R_{sL_1}+\dfrac{1}{jC_1\omega} & \dfrac{M_{12}(z,x)}{L_{p2}} \\ -\dfrac{M_{12}(z,x)}{L_{p2}} & \dfrac{1}{jL_{p2}\omega}+jC_2\omega+\dfrac{1}{R_2} \end{pmatrix} \quad (5)$$

SPICE-BASED ELECTRICAL MODELING OF COILS

The mutual inductance of two loop-shaped air coils whose axes are parallel (radius a for emitter and external radius b for receiver, coil distance z, distance between the axes x) can be expressed by the double integral of Neumann's Eq. 6 :

$$M_{12}=\frac{\mu_0}{4\pi}\iint_{1\ 2}\frac{\overrightarrow{dl_1}\overrightarrow{dl_2}}{r} \quad (6)$$

In which by replacing the cartesian coordinates of points P_1 and P_2 and their elementary displacements dl_1 and dl_2, the solved equation of the mutual inductance is given by Eq. 7. Eisthewire thickness, only consideredin the rigorous calculation of the mutual inductance (Chaoui *et al*., 2002, 2003, 2005; Galbraith *et al*., 1987):

$$M_{12}(z,x)=\sum_{i=0}^{N_1-1}\frac{\mu_0}{4\pi}\int_{10.2.\pi}^{15.2\pi}\int_{0}^{2\pi}\frac{ar_2(\sin(\phi-\theta)+\phi\ \cos(\theta-\phi))\ d\theta\ d\phi}{\sqrt{\begin{matrix}x^2+a^2+(r_2\phi)^2+\left(z+\dfrac{E}{2}+iE\right)^2+\\ 2(r_2\phi)x\ \cos\ \phi-2ax\ \cos\theta-\\ 2a(r_2\phi)\ \cos(\theta-\phi)\end{matrix}}} \quad (7)$$

It is sometimes more current to use the concept of the factor of coupling factor k which is adapted, generally more as parameter of design because it does not depend on the number of coil turn of this fact the analysis will be a little simpler. Most of the literature uses this factor like state of the art to describe the coupling between the two coils without to have thought of misalignments and the coil shape which them even give rise to this coupling. Therefore, much of the aforementioned researchers choose a coupling factor K ranging between 0.1 and 0.3, really this imposes the mutual inductance by relation:

$$k(z,x)=\frac{M_{12}(z,x)}{\sqrt{L_1L_2}}$$

On the other hand, the mutual inductance was to be caused and measured for the shapes and positions given of the coils. Conversely, this study expresses M directly according to displacements (x, z) for the case of a solenoid as an emitter and an Archimedes coil as a receiver. Then, a polynomial interpolation of the mutual inductance is obtained with Matlab®.

The last step consists in integrating this mutual inductance M(x, z) which is given by the polynomial function, into an equivalent PSpice model which will be stored into the OrCAD library. The 4th order interpolation equations of the mutual inductance Eq. 7 as a function of longitudinal displacement z for different lateral displacement x = 2, 4, 6 and 8 mm are given, respectively by Eq. 8-11:

$$M_{12}(z,x)=-2.2471\cdot z^4+8.0403\cdot10^{-2}\cdot z^3-6.8497\cdot10^{-4}\cdot z^2-6.7224\cdot10^{-6}\cdot z^1+127.03\cdot10^{-9}.z^0 \quad (8)$$

$$M_{12}(z,x)=-1.1333\cdot z^4+3.1015\cdot10^{-2}\cdot z^3+1.1071\cdot10^{-4}\cdot z^2-12.071\cdot10^{-6}\cdot z^1+137.44\cdot10^{-9}z^0 \quad (9)$$

$$M_{12}(z,x)=2.2327\cdot z^4-1.0185\cdot10^{-1}\cdot z^3+1.954\cdot10^{-3}\cdot z^2-2.2276\cdot10^{-5}\cdot z^1+151.84\cdot10^{-9}.z^0 \quad (10)$$

$$M_{12}(z,x)=1.9306\cdot z^4-9.124\cdot10^{-2}\cdot z^3+1.8049\cdot10^{-3}\cdot z^2-2.0710\cdot10^{-5}\cdot z^1+139.16\cdot10^{-9}.z^0 \quad (11)$$

The equivalent OrCAD PSpice diagram of the inductive link is represented in Fig. 3. Figure 4 shows the results obtained with OrCAD for the mutual inductance of the inductive link as a function of the longitudinal displacement z for various lateral displacements (x = 2, 4, 6, 8 mm).

The x axis is labeled in mV instead of mm because of OrCAD's limitations (model inputs must be expressed in voltages or currents). The results of the mutual inductance calculated with Eq. 8 are identical to those interpolated up to z = 16 mm for each x.

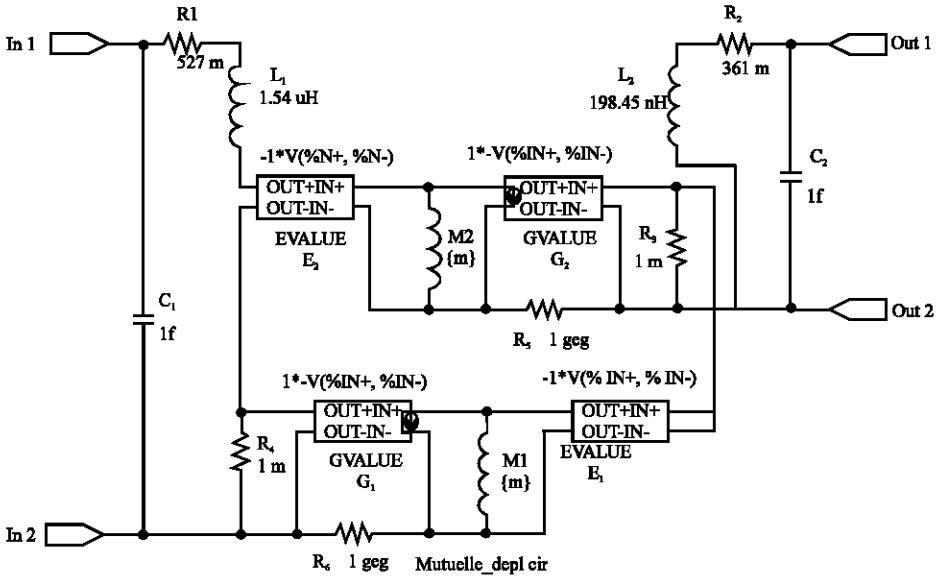

Fig. 3 : Equivalent OrCAD PSpice model of the inductive link

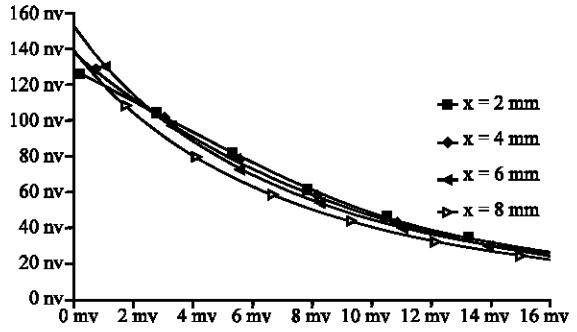

Fig. 4: Mutual inductance (interpolated polynomials) vs. longitudinal displacement (z) and for various side displacements (x = 2, 4, 6, 8 mm) – 1 mV represents 1 mm

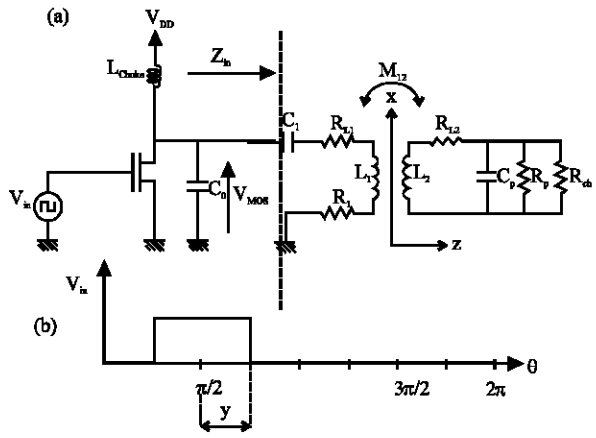

Fig. 5: (a) Class E amplifier loaded by the inductive link, (b) chronogram of transistor switching

CLASS E COIL DRIVER FOR THE TRANSCUTANEOUS INDUCTIVE LINK

Figure 5a shows the schematic of the class E amplifier loaded by the inductive link and Fig. 5b the switching chronogram of the transistor. A 2.3 ratio between the external and the internal coil was selected (reducing the minimum alignment deviation and ensuring a good stability). The external coil is the one shown in Table 1. Since, the signal is periodic only one period is considered for circuit simulation with $\theta = \omega t$ ($0 \le \theta \le 2\pi$). The model chosen for the inductive link is the one given by the interpolated polynomial equations. This model is implemented electrically via electrical simulations performed on OrCAD. The model presented by Zierhofer and Hochmair (1990), although not bringing any advantage in terms of simplicity or accuracy, makes it possible to study the performance of the class E amplifier when it is loaded by an inductive link with variable coupling (variable displacement). Then, the use of Raab (1978) requires the knowledge of the output impedance. It can be noticed that only the load resistance and inductance of the class E circuit depend on relative displacements (z, x) and on frequency. By taking into account, the equivalent model of the transponder's reflected impedance, the structure in Fig. 5 can be represented by the simpler schematic in Fig. 6. In order to come down to the usual structure of the class E amplifier,

resistance R and inductance L are replaced, respectively by R(f, z, x) (Eq. 13) and L(f, z, x) (Eq. 14). R(f, z, x) and L(f, z, x) themselves depend on frequency and displacements. Where:

$$Z_{in}(f,z,x)=\frac{V_{in}}{I_1}=\frac{\det(H(f,z,x))}{h_{22}} = R(f,z,x)+j\omega L(f,z,x) \quad (12)$$

$$R(f,z,x)=R_1+R_{L1}+\frac{M(z,x)^2}{L_2^2}\cdot\frac{1}{1+\left[Q_r\frac{\omega_r}{\omega}((\frac{\omega}{\omega_r})^2-1)\right]^2}.R_2 \quad (13)$$

$$L(f,z,x)=L_1\left[1-\frac{M(z,x)^2}{L_1L_2}\right]-\frac{\frac{M(z,x)^2}{L_2}Q_r^2(\frac{\omega_r}{\omega})^2\left[(\frac{\omega}{\omega_r})^2-1\right]}{1+\left[Q_r\frac{\omega_r}{\omega}((\frac{\omega}{\omega_r})^2-1)\right]^2} \quad (14)$$

Several models were introduced by Sokal and Sokal (1975), Raab (1977), Kazimierczuk and Puczko (1987) and other researchers to describe the behavior of the class E amplifier each one with its advantages and disadvantages. The main advantage of the first two models is to lead to simple dimensioning equations. Therefore, they make it possible to determine the influence of conduction time 2y (Fig. 5b) on circuit performance under ideal operation. However, the most critical assumption of these simplified models deals with the quality factor of the load, the series capacitor C_1 and the shunt capacitor C_0. Conversely, Kazimierczuk and Puczko (1987)'s model, considered among the most complicated does not make use of this assumption. The researchers clarify the inaccuracy of the simplified model for low values of the quality factor. All these models cannot be used out-of-the-box because the theoretical efficiency is expressed as a function of the coupling factor K and not of displacements. Consequently, the quality factor is computed using displacements and either model is used depending of this factor. Capacitance values C_0 and C_1 calculated to (Sokal and Sokal, 1975) make it possible to ensure correct class E operation. Indeed, the optimum operation of an amplifier in class E sets two constraints on drain waveforms: the drain Voltage VMOS(t) must be equal to zero when the transistor is conductive and the voltage rise must be delayed until the transistor is completely blocked. When these two constraints are met for given parameters and displacements, proper class E operation is obtained. Then, the output voltage at the load is purely sinusoidal with 10 V maximum value. Moreover, it is necessary to assess the sensitivity of the class E amplifier to the variation of circuit parameters since, it makes it possible to set device

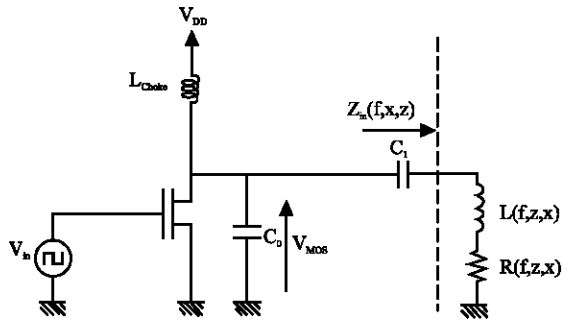

Fig 6: Class E amplifier with the impedance reflected by the inductive link

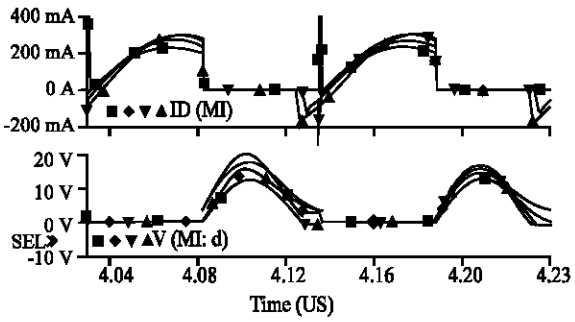

Fig 7: Waveforms of the class E amplifier loaded by the inductive link for x = 0 and different longitudinal displacements (z = 4, 6, 8, 10 mm): drain current (top) and drain-source voltage (bottom)

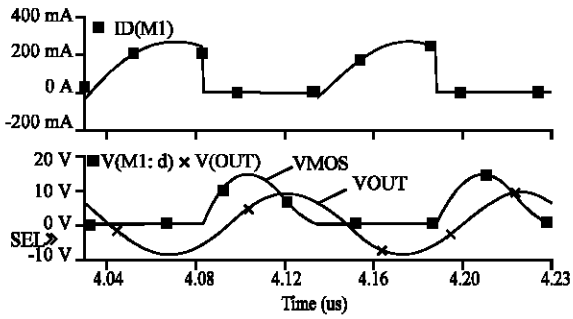

Fig 8: Waveforms of the class E amplifier loaded by the inductive link for x = 0 and z = 6 mm: drain current (top), drain-source voltage and voltage across the load

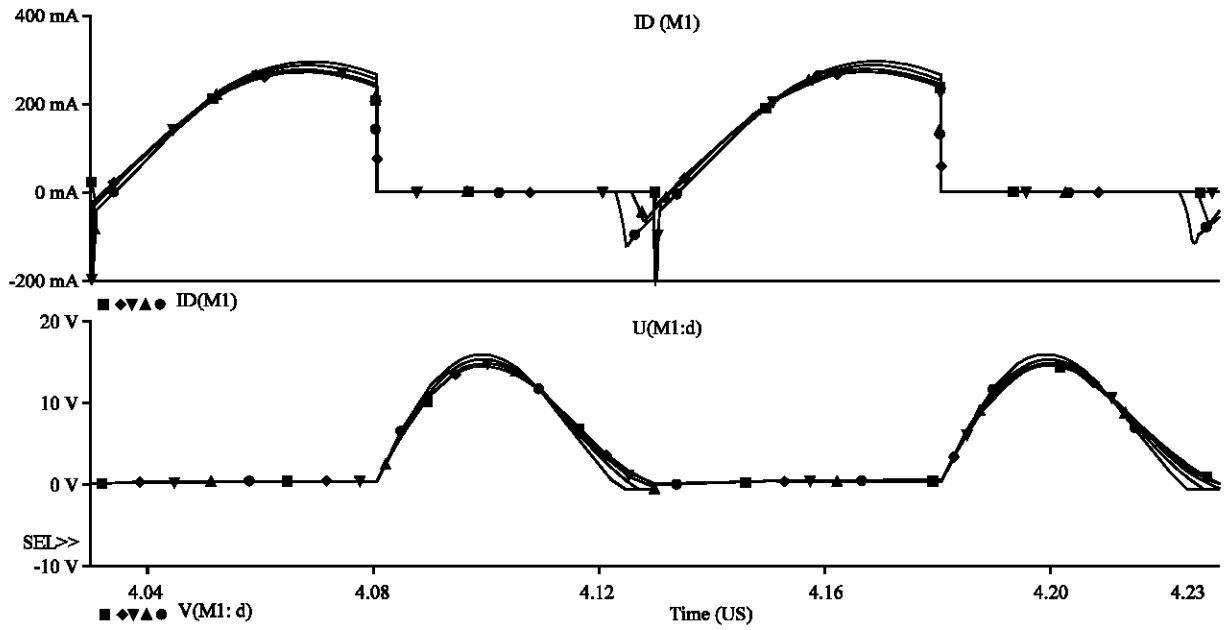

Fig. 9: Waveforms of the class E amplifier loaded by the inductive link for z = 0 and different lateral displacements (x = 0, 2, 4, 6, 8 mm): drain current (top) and drain-source voltage (bottom)

tolerances and to predict the operating mode of the amplifier under non ideal conditions. The analysis shown in Fig. 7 is necessary for the determination of the behavior of the amplifier with an arbitrary set of longitudinal displacements (z = 4, 6, 8, 10 Voltage VMOS(t) of the drain-source can now be expressed for both halves of the period by Eq. 15 and 16. The whole system was also simulated through OrCAD. Simulation results are shown in Fig. 8 a very large mm) for the same condition of ideal positioning, i.e., the same capacitors C_0 and C_1. In this study, all the simulation results are given by using the PSpice macromodel (OrCAD) proposed by the model shown in Fig. 3. The difference is observed in the computing time.

The basic data characterizing the class E operating mode when loaded by the inductive link are transistor drain current and voltage ID(t) and VMOS(t). These results and the voltage across the load are simulated for a zero lateral displacement and a 6 mm longitudinal distance. Likewise and under the same analysis conditions, Fig. 9 shows the resultants obtained for lateral displacements (x = 0, 2, 4, 6, 8 mm). A drift in the waveforms can be observed when either displacement increases since, optimal circuit values computed for x = z = 0 cannot ensure that the amplifier operates in class E in any experimental condition. Therefore, these displacements slightly reduce the amplifier's yield. The optimal solution to this issue would require capacitance values to be computed again for each displacement. The results of the class E amplifier operating at 10 MHz demonstrate a transmission yield above 80% and the global efficiency (transmission + link + reception) of power transfer is close to 35%. In terms of sensitivity to misalignment, results show a good stability. These results can be linked to the appropriate choice of the coil shapes and geometries but remain valid only for small displacements.

VOLTAGE REGULATION AT THE SECONDARY WINDING

Apart from the effect on the voltage converter's operating regime, the variation of drain voltage caused by displacements also leads to a change in the voltage induced on the secondary winding. The use of a single internal voltage regulator may solve this issue but the efficiency of such devices is about 90% and they will generate significant losses in the secondary circuit. Therefore, a better solution relies on rectification.

Figure 10 shows the schematic of a voltage rectifier which replaces R_{ch} (Fig. 5a) to deliver a continuous and stable tension for various displacements (i.e. for any variation of the supply voltage). The rectifier is a single loop made up of four transistors (two NMOS and two PMOS) (Tsai *et al*., 2004). The positive terminal of the output is connected to a large filtering capacitor C_L while the negative terminal is forced to the ground. C_L is used to smoothen the ripple. Simulation results are shown in

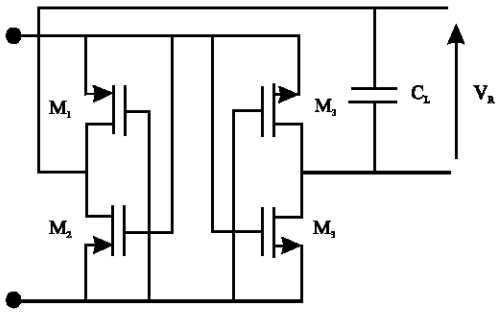

Fig. 10: Electrical schematic of the voltage rectifier

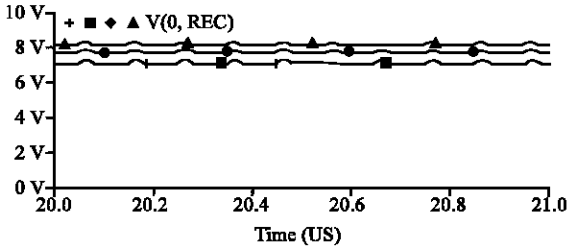

Fig. 11: Output waveform of the rectifier for different lateral displacements (x = 2, 4, 6, 8 mm)

Fig. 11 for various lateral displacements. As can be seen, the output voltage is around 7-8 V for various longitudinal displacements with only a small ripple. It is given as a function of displacements and not of coupling factors. However, the DC value is not constant therefore, an additional regulation stage is necessary in order to power the internal part of the implant.

CONCLUSION

In this study, a theoretical study of an inductive link driven by a class E power amplifier was presented. Modeling the inductive link with a PSpice macromodel (OrCAD) made it possible to express the characteristics of the load circuit of the amplifier in terms of longitudinal and lateral displacements. This makes it easier to simulate the behavior of the whole link. The fixed-frequency class E amplifier on which this study is based, improves power efficiency, provided that lateral and longitudinal displacements are low enough not to push the amplifier outside of its class of operation. It can be seen that if one displacement is fixed while the other varies in small proportions (<8 mm), the equivalent elements of the load and the global efficiency vary only slightly. If a displacement rises >8 mm, the efficiency of the link is reduced according to the distance of both coils. A considerable change can be observed in amplifier waveforms above this limit, corresponding to out-of-class operation. A further improvement of the system would consist of an automatic adjustment of the operating frequency in order to ensure the best efficiency. The reserchers are currently working on this feature.

REFERENCES

Catrysse, M., B. Hermans and R. Puers, 2004. An inductive power system with integrated bi-directional data-transmission. Sensors Actuators: A. Phys., 115: 221-229.

Chaoui, M., H. Ghariani, M. Lahiani and F. Sellami, 2002. Maximum of mutual inductance by inductive link. Proceedings of the 14th IEEE International Conference on Microelectronics, Dec. 11-13, Grenoble, France, pp: 265-268.

Chaoui, M., H. Ghariani, M. Lahiani and F. Sellami, 2003. Optimization of the output of energy transfer in the system implantabless. Proceedings of the 7th IEEE International Conference on Intelligent Engineering Systems, (ICIES'03), Assiut Luxor, Egypt, pp: 572-575.

Chaoui, M., H. Ghariani, M. Lahiani, R. Perdriau, M. Ramdani and F. Sellami, 2005. Stability electrical modeling of inductive link for high energy transmission. Proceedings of the 12th IEEE International Conference on Electronics, Circuits and Systems: ICECS, Dec. 11-14, Gammarth, Tunisia, pp: 5-8.

Galbraith, D.C., M. Soma and R.L. White, 1987. A wide-band efficient inductive transdermal power and data link with coupling insensitive gain. IEEE Trans. Biomed. Eng., 34: 265-275.

Kazimierczuk, M.K. and K. Puczko, 1987. Exact analysis of class E tuned power amplifier at any Q and switch duty cycle. IEEE Trans. Circuits Syst., 34: 149-159.

Raab, F.H., 1977. Idealized Operation of the class E tuned power amplifier. IEEE Trans. Circuits Syst., 24: 725-735.

Raab, F.H., 1978. Effects of circuit variations on the class E tuned power amplifier. IEEE J. Solid-State Circuits, 13: 239-247.

Sokal, N.O. and A. Sokal, 1975. Class E-A new class of high-efficiency tuned single-ended switching power amplifiers. IEEE J. Solid-State Circuits, 10: 168-176.

Tsai, C.C., S.B. Dai, W.T. Lee and T.Y. Lee, 2004. The RF circuit design for magnetic power and data transmission. Proceedings of the International Conference on Information Technology and Applications (ICITA 2004), Paper 56-5, Jan. 2004.

Vandevoorde, G. and R. Puers, 2001. An inductive energy transfer for stand-alone systems: A comparison between low and high power applicability. Elsevier Sensors Actuators, 92: 305-311.

Zierhofer, C.M. and E.S. Hochmair, 1990. High-efficiency coupling-insensitive transcutaneous power and data transmission via an inductive link. IEEE Trans. Biomed. Eng., 37: 716-722.